ARMY RESEARCH LABORATORY

Bio-mimetic Millimeter-scale Flapping Wings for Micro Air Vehicles, Year II

by Christopher Kroninger, Jeffrey Pulskamp, Ronald G. Polcawich, and Eric Wetzel

NOTICES

Disclaimers

The findings in this report are not to be construed as an official Department of the Army position unless so designated by other authorized documents.

Citation of manufacturer's or trade names does not constitute an official endorsement or approval of the use thereof.

Destroy this report when it is no longer needed. Do not return it to the originator.

Army Research Laboratory

Aberdeen Proving Ground, MD 21005

Bio-mimetic Millimeter-scale Flapping Wings for Micro Air Vehicles, Year II

Christopher Kroninger
Vehicle Technology Directorate, ARL

Jeffrey Pulskamp and Ronald G. Polcawich
Sensors and Electron Devices Directorate, ARL

and

Eric Wetzel
Weapons and Materials Research Directorate, ARL

REPORT DOCUMENTATION PAGE

1. REPORT DATE *(DD-MM-YYYY)*	2. REPORT TYPE	3. DATES COVERED (From - To)	
April 2010	DRI		

4. TITLE AND SUBTITLE	5a. CONTRACT NUMBER
Bio-mimetic Millimeter-scale Flapping Wings for Micro Air Vehicles, Year II	
	5b. GRANT NUMBER
	5c. PROGRAM ELEMENT NUMBER

6. AUTHOR(S)	5d. PROJECT NUMBER
Christopher Kroninger, Jeffrey Pulskamp, Ronald G. Polcawich, and Eric Wetzel	
	5e. TASK NUMBER
	5f. WORK UNIT NUMBER

7. PERFORMING ORGANIZATION NAME(S) AND ADDRESS(ES)	8. PERFORMING ORGANIZATION REPORT NUMBER
U.S. Army Research Laboratory ATTN: RDRL-VTU Aberdeen Proving Ground, MD 21005	ARL-TR-5184

9. SPONSORING/MONITORING AGENCY NAME(S) AND ADDRESS(ES)	10. SPONSOR/MONITOR'S ACRONYM(S)
	11. SPONSOR/MONITOR'S REPORT NUMBER(S)

12. DISTRIBUTION/AVAILABILITY STATEMENT

Approved for public release; distribution unlimited.

13. SUPPLEMENTARY NOTES

14. ABSTRACT

The focus of this Year II Director's Research Initiative resulted in design improvements and extended experimental capability for the next design iteration of millimeter-scale flapping wings. Three different design approaches intended to produce significant pitching motion through a flap stroke are outlined while providing a more detailed description of the design methodology for one technique employing two orthogonally mounted bending actuators. Two possible approaches to designing a balance that will allow for unobtrusive measurements of the wing force production demonstrate the necessary sensitivity. A described meso-fabrication setup will reduce design cycle time. Finally, a nearly capable Reynolds number-scaled testing facility, which will assist in future designs and experimental assessment, is briefly described.

15. SUBJECT TERMS

MEMS, micro air vehicles, robotics, flapping wings, meso-fabrication, Reynolds number, oil

16. SECURITY CLASSIFICATION OF:			17. LIMITATION OF ABSTRACT	18. NUMBER OF PAGES	19a. NAME OF RESPONSIBLE PERSON
a. REPORT	**b. ABSTRACT**	**c. THIS PAGE**	UU	20	Christopher Kroninger
Unclassified	Unclassified	Unclassified			**19b. TELEPHONE NUMBER** *(Include area code)* (410) 278-5690

Contents

List of Figures

List of Tables

Acknowledgments

INTENTIONALLY LEFT BLANK.

1. Objective

The objective of the proposed research is to develop millimeter-scale flapping wings, created through a Micro-Electro-Mechanical System (MEMS) process, that produce lift and flight characteristics similar to those of insects in the same size class. Progress towards this objective includes a study of materials, MEMS design and processes, and wing aeromechanics for a prototype legged MEMS architecture already under development. Building on the first year's success, which revealed flapping with a range of angular motion of about 30–50° (*1*), the main objective of Year II explores both active and passive pitch control mechanisms to provide a more complete replication of insect flight kinematics to generate highly efficient lift during the entire wing stroke. In addition, new device fabrication techniques are developed and demonstrated to drastically reduce design cycle times and speed device evaluation and optimization.

2. Approach

2.1   Wing/Actuator Designs

Previous Year I designs exhibited significant flapping motion while lacking the complimentary pitching or twisting motion necessary to place the wing at an angle of attack (AoA) relative to its flapping motion. Several actuator concepts to be tested are expected to provide greater actuator pitch authority. Figure 1 shows the concepts explored, which include two active actuation concepts and a passive pitching concept. The concept in figure 1a relies on two orthogonally oriented bending actuators, which will drive motion nearly independently along the flapping and pitching axes. In the conceptual illustration, the most exterior actuator induces pitching of the wing along an axis parallel to the span of the wing. The interior actuator causes flapping within the pitching frame of reference, meaning that the flap stroke will not be contained within the stroke plane. A second variation on this concept has also been implemented, where the arrangement of the bending and pitching actuators have been switched resulting in flapping restricted to the stroke plane and pitching remaining along the spanwise axis. The concept of a pitch hinge has been demonstrated by Wood (*2*). In his case, a large flap (~90% of the chord) was passively pitched at the end of each half wing stroke setting the appropriate AoA for the next half stroke. Figure 1b illustrates an active version of this design, where part of the span length wing hinge consists of a lead zirconate titanate (PZT) bending actuator. This hinge mechanism actively pitches the wing throughout the flap stroke while flapping is maintained within the stroke plane. The final concept in figure 1c is the use of an entirely passive hinge. This design is what Wood (*2*) has done and the concept has been applied by itself and in conjunction with the other actuator designs. Combinations of all three core designs have been included in the current prototype runs. The design of the basic wing/actuator system is

illustrated in figure 2 with a planform view on the top and a slice through the cross section "a- - - a" (in the figure), revealing the layers that make up the devices. The actuator design consists of a PZT layer offset from the neutral axis of the beam, which results in the beam bending when the layer compresses.
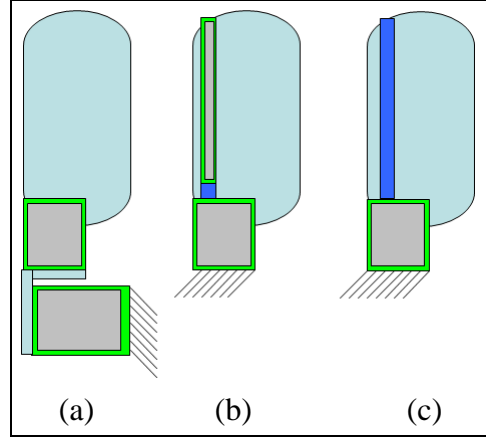

Figure 1. Conceptual images of actuator designs: (a) two orthogonal vertical actuator design, (b) actuated hinge design, and (c) passive rotation concepts.
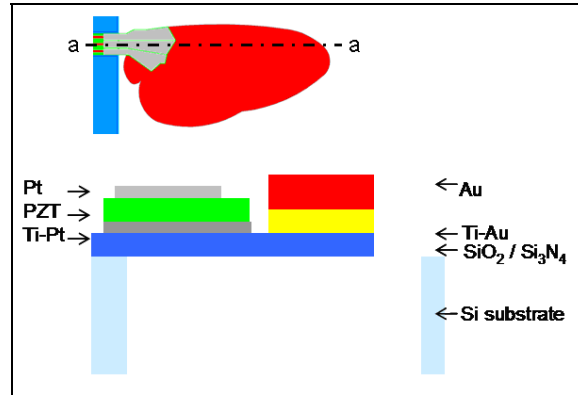
Figure 2. Top view and cross-sectional slice illustrating the material composition of the wing/actuator design.

A basic static analysis of the actuator/wing designs has been performed for each concept. For the case of the two orthogonally oriented actuators, the results of the static actuator tip rotation for varying actuator lengths can be seen in figure 3 with different curves for varying actuator thicknesses. Figures 3a and 3b represent actuators of 300 and 500 µm width, respectively. As can be seen in table 1, this analysis is for a 2-mm span wing/actuator system experiencing a static aerodynamic load at the center of pressure of the wing. The analysis of the actuator itself is performed with a beam theory model, which is nonlinear in the sense of incorporating large curvatures (i.e., no small angle assumption). Along with the point loading of the anticipated aerodynamic load, the contraction of the PZT element induced a distributed bending moment

across the surface of the beam. Exploring the range of possible actuator sizes in figure 3a, it is apparent that for the 300-µm wide beam, the 1-µm-thick silicon dioxide (SiO$_2$) layer beam provides a maximum of 3º of tip deflection of about 250-µm span; beyond this length the actuator looses the authority to overcome the aerodynamic load on the wing. The design problem equates to matching the mechanical impedance of the actuator/wing system to the ratio of the aerodynamic load to the desired wing speed at the location of the center of pressure. The mechanical impedance is a strong function of the thicknesses and, to a lesser extent, the lateral dimensions. The selection of the thickness of the SiO$_2$ must be consistent across the entire device because of constraints of the fabrication process. Therefore, for a given aerodynamic load, the thickness of both actuators is traded with the lateral dimensions for various combinations of device size and wing velocity (lift). The analysis suggests that larger wing sizes require thicker actuators, and consequently, larger actuator dimensions to handle the larger dynamic loads with the same kinematic performance.
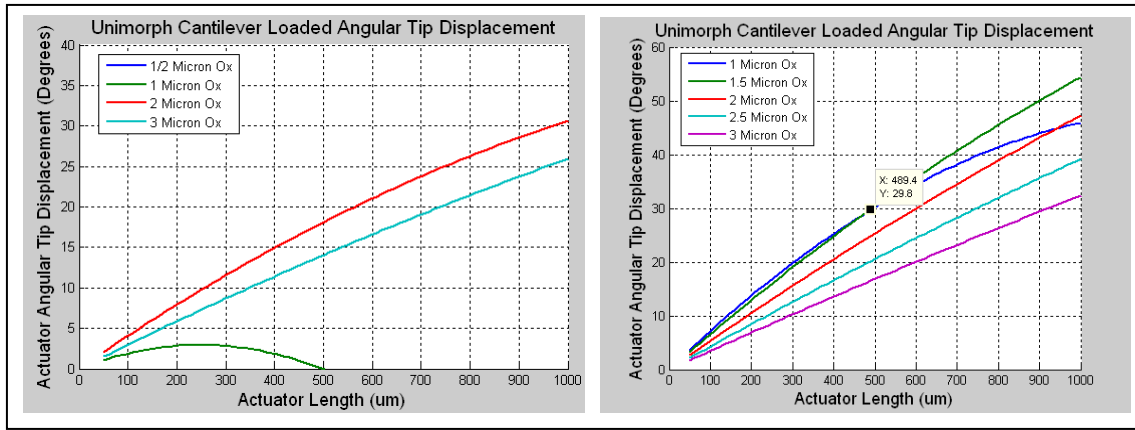

Figure 3. Static actuator tip rotation of varying lengths and thicknesses for an aerodynamically loaded wing: (a) 300-µm-wide actuator and (b) 500-µm-wide actuator.

Table 1. Characteristics of the wing/actuator system.

Wing Span (mm)	2
PZT Thickness (µm)	0.5
Electrode Thicknesses (Å)	800 & 300
SiO$_2$ Layer (µm)	0.5, 1.0, 2.0 & 3.0
Center of Pressure	2/3 span from root, 1/3 chord from tip
Aerodynamic Load (µN)	12
Inertial Load (µN)	0

The mode of operation of the actuator providing the flapping is designed to be different from that of the one driving the pitching motion. The flapping has been designed to take advantage of resonant excitation to achieve a significant flapping motion, as the insect kinematics for this degree of freedom map well to a sinusoid. Therefore, design options for the flap actuators can be viewed from the perspective of their dynamic response. Table 2 includes the bending actuator design options assuming a quality factor of five times the static response, a reasonable

3

assumption based on experience with prior devices and expectations of system efficiency. The length of the actuator was chosen to achieve ±70º of angular flap deflection, which is similar to that seen in the model insect the fruit fly (*3*). The desired pitching kinematics do not map well to a sinusoid. Consequently, the pitching of the wing is designed to be controlled directly, taking no advantage of resonance; therefore, the static deflection must at least equal the desired dynamic deflection. The chosen dimensions in table 2 for the pitch actuator were selected to achieve ±25º of pitch or an AoA of 65º through the flap stroke. Confirmation of these results was also performed using a finite element analysis (FEA). Estimates of actuator response time were also obtained through the use of FEA model analysis and were compared to the desired (insect-inspired) kinematics to ensure the chosen dimensions of actuator/wing system were capable of meeting the response time requirements. A similar methodology was applied to the other two actuator concepts.

Table 2. Actuator designs.

Actuator	Flap	Pitch
Length (µm)	370	500
Width (µm)	300	500
Height (µm)	2	2
Static Deflection (º)	14	25
Dynamic Deflection (º)	70	–

2.2   Balance Design

Although the measure of the force production can be inferred from the motion of the wings with the use of aerodynamic and structural numerical models, a reliable direct measure of loads is a second objective of this work. Two measurement techniques were explored to achieve this objective, an external balance and a design integrated into the actuators themselves. In order to achieve even useful average force measurements of lift, a minimum of 12 µN must be resolvable.

2.3   External Balance Design

The design and use of an external balance for measuring loads this small is plagued with potential difficulties. The primary motivation for pursuing such a device is that a single calibration can be performed that is applied to the measurement of all devices. A commercially available device has been identified, which, with some modification, is capable of achieving the necessary force resolution for a single axis measurement. The active element of this device is a 5-mm rectangular silicon (Si) beam of 150 µm in thickness. A strain gage on the upper and lower surfaces allows the bending moments in the beam to be measured. The gage was rated for a maximum measurement of tip force as high as 120 mN, well above the expected range of 12 µN. We found it necessary to extend the moment arm of the Si beam to improve the force resolution.

4

2.4   Integrated Balance Design

A second concept explored for making direct load measurements of the wings is illustrated in figure 4. High aspect ratio rectangular PZT elements, identical in composition to the actuators but electrically isolated, can serve as sensors by measuring their voltage response to strain. Cuts through the thickness of the actuator on the sides of the sensors ensure the piezoelectric sensing is largely due to the long axis of the sensor. Hence, orthogonal sensors should be able to resolve orthogonal strain responses, providing decoupled sensing of the strains. Making the assumption that all the strain experienced by the actuator is due to bending, a relationship relating the load at of the end of the actuator and the voltage across the sensor can be formulated. The sensor area can be sized to ensure that a sufficiently large output voltage is achieved at the desired minimum force. The minimum desired force and resolvable voltage are 1.5 nN and 100 µV, respectively.
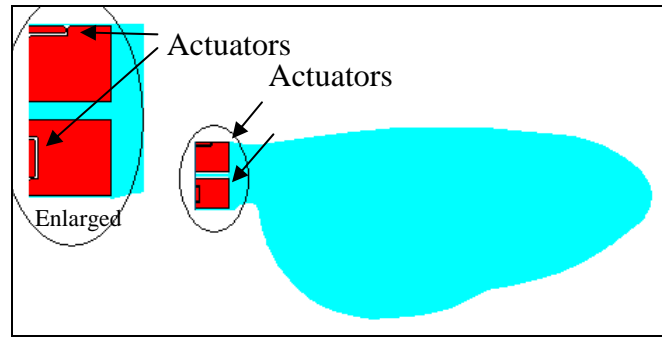

Figure 4. Integrated actuator concept.

This design is advantageous in that the actuator is incorporated right into the design and fabrication of the devices, thus eliminating additional handling/mounting concerns associated with an external balance. Drawbacks to this design include the fact that each device has to be calibrated individually, which we envision will be performed using an atomic force microscope. This calibration is further complicated by the coupling it will experience with the applied bending moment of the adjacent actuator element. Calibration will need to be performed over a range of wing loadings for each actuation load.

2.5   Meso-fabrication

The lithographic techniques used to fabricate the current prototypes enable the construction of highly precise, complex devices at very low cost when produced in large quantities. However, for the current design effort, the high complexity and cost, long turnaround times (averaging 6 months per batch), and high failure rates of lithographic manufacturing drastically limit our ability to iteratively design and improve devices.

To address this shortcoming, an alternative fabrication approach was explored. The concept is to use lithographic processes to create an array of cantilevered piezoelectric actuator "stubs" without attached wings. These actuators can be produced with reasonably high repeatability due to their simple design. Then, as a separate process, wings are fabricated and attached to the

piezoelectric stubs to create a complete flapping system. The advantage of this approach is that it decouples wing and actuator manufacturing steps, speeding up the design cycle times and allowing for greater design freedom and iterations.

Figure 5 shows the micromanipulation system constructed for mesoscale fabrication. A series of precision linear and rotational stages are used to position subcomponents. A vacuum chuck is used to grab and release subcomponents. Ultraviolet (UV)-curable adhesives, cured with a fiber optically coupled UV light source, are used to bond the subcomponents. Figure 5b (inset) shows an example part made by precisely rotating and aligning a wing and bonding it to a Si wafer substrate.
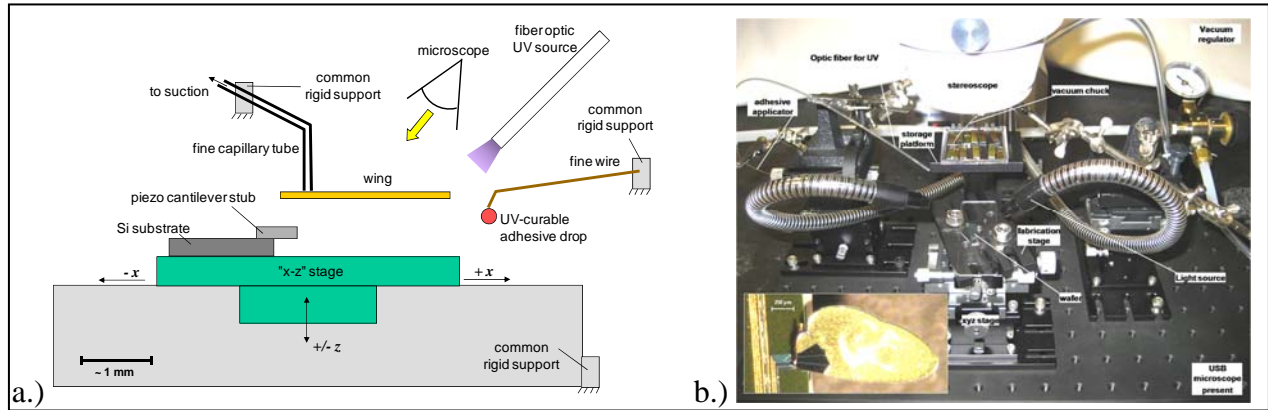

Figure 5. (a) Schematic and (b) photo of micromanipulator for mesoscale device fabrication. The inset shows example of a wing attached to a Si wafer.

2.6   Reynolds Number-scaled Oil Tank

In a further effort to increase the speed of design turnaround, a facility capable of yielding aerodynamically similar performance of larger-scale, slower flapping wings has been produced. This provides the capability of assessing the effectiveness of various design parameters prior to implementation at actual size in the lithographic or meso-fabrication technique. These assessable parameters include features such as the details of the flap stroke (flap and pitch angles and rates) and the wing planform design. Assessment comparisons of performance are established with force balance measurements.

3.   Results

Currently, the first devices of these designs are being fabricated. Completion and packaging of the devices is expected to be completed in early 2010.

In order to assess the potential performance of the external balance, an attempt was made to calibrate the device at loads on the order of single microNewtons (or tenths of milligrams), which is the coarsest resolution allowable to achieve useful results. Calibration loads consisted

of lengths of 51-µm-diameter stainless steel wire. Knowing the density, diameter, and length of the wire, the weight can be inferred. During a measurement, the masses were hung across a hook at the end the beam and then the entire mechanism was enclosed to avoid disturbance from turbulence.

The two strain gages on the beam were wired into a half bridge circuit. The circuit was excited with a filtered 5 V and the voltage across the bridge was filtered at 8 kHz, amplified by a factor of 512 and sampled at a rate of 102.4 kHz for 1280 samples. At each calibration weight, five samples were recorded prior to moving on to the next weight. Results of the same procedure collected over three different days are shown in figure 6 along with a best fit line applied to each sample. It is clear that over the three-day span there was a drift in the offset, which could be related to many factors including changes in temperature, humidity, or dust settling on the balance. Despite this, the slopes of the curves are consistent between successive days, a condition that is necessary for this application. High precision in the measurement is evident in that the scatter is also quite minimal between repeated measurements. This sensor should be sufficient for measuring the variation of force over a period of motion. Although this is a static test of the actuator, it can be assumed that the sensor will work well dynamically as long as the primary natural frequency of the sensor/wing system remains above the dynamic response of the wing. The predicted primary resonance frequency of the extended beam sensor is about 1.2 kHz compared to the desired frequency of 200-Hz flapping. Care will need to be taken to ensure that this natural frequency does not drop significantly with the addition of the wing to the end of the beam.
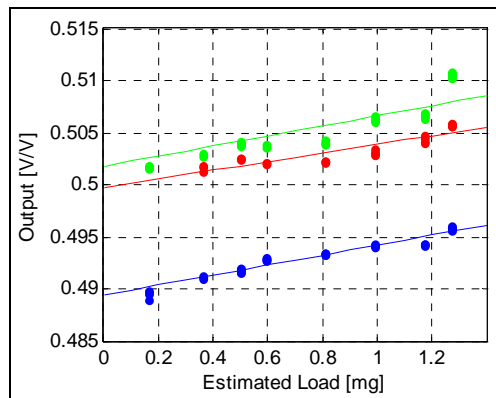

Figure 6. Calibration curves of external beam loading.

Application of the sensor has several limitations. First, it will be a coarse measurement relative to the expected performance of the integrated balance. It will also only yield a single axis of measurement at a time, meaning lift and drag cannot be measured simultaneously, rather the wing must be reoriented relative to the sensor to capture each axis. Handling and mounting the wings to such a device will not be a trivial task, requiring a redesign of the wing packaging. The external balance may prove most useful as a means of calibrating the integrated balance in real time rather than performing a separate calibration.

7

4. Conclusions

The work over the course of the last year has continued to move the project toward its primary objective of achieving lift production similar to that of an insect. While drawing conclusions regarding the performance of the new wing designs in terms of the flap/pitch performance or the performance of the integrated balance will have to wait until the fabrication and packaging can be completed, based on the success of the previous designs, we anticipate that the new designs will demonstrate significant motion in both flap and pitch, the two required motions to generate hovering insect-like flight. Alternative fabrication approaches are also under consideration and may accelerate the prototyping process. The two balance concepts have limitations in their implementation but both have the potential for yielding useful data. The work continues to suggest the aims of effort will be achieved.

5. References

1. Bronson, J.; Pulskamp, J.; Polcawich, R.; Kroninger, C.; Wetzel, E. Thin Film PZT Flapping Wing Actuators for Insect-Inspired Robotics. *22nd IEEE International Conference on MEMS*, Sorrento, Italy, January 2009.

2. Wood, R. The First Takeoff of a Biologically Inspired At-Scale Robotic Insect. *IEEE transactions on robotics* **2008**, *24* (2).

3. Sane, S. P.; Dickinson, M. H. The Control of Flight Force by a Flapping Wing: Lift and Drag Production. *J. Exp. Biology* **2001**, *204*, 2607–2626.

6. Transitions

It is anticipated that this endeavor will be incorporated into the regular mission of the U.S. Army Research Laboratory (ARL) and continue as a multi-Directorate effort. Progress toward our original objective will be our goal. We hope to eventually met this objective, demonstrating not only that force measurement within the test stand structure can demonstrate equivalent lift production to an insect, but also that tethered lift-off of a device similar to the one demonstrated by Wood (*2*) can be achieved.

The following two conference presentations have been made regarding this work:

1. Bronson, J.; Pulskamp, J.; Polcawich, R.; Kroninger, C.; Wetzel, E. Thin Film PZT Flapping Wing Actuators for Insect-Inspired Robotics. *22nd IEEE International Conference on MEMS*, Sorrento, Italy, January 2009.

2. Kroninger, C.; Pulskamp, J.; Polcawich, R.; Bronson, J.; Wetzel, E. Design and Characterization of Millimeter-Scale Flapping Wings. *AHS International 65th Annual Forum & Technology Display*, Grapevine, TX, May 2009.

List of Symbols, Abbreviations, and Acronyms

AoA   angle of attack

ARL   U.S. Army Research Laboratory

FEA   finite element analysis

MEMS Micro-Electro-Mechanical System

PZT   lead zirconate titanate

Si   silicon

SiO_2 silicon dioxide

UV   ultraviolet